ACS OMEGA

Open Access

http://pubs.acs.org/journal/acsodf

Article

Design and Exploration by Quantum Chemical Analysis of Photosensitizers Having [D−π−π−A]- and [D-D-triad-A]-Type Molecular Structure Models for DSSC

Ankit Kargeti, Rudra Sankar Dhar,* Shamoon Ahmad Siddiqui, and Na'il Saleh*

Cite This: *ACS Omega* 2024, 9, 11471−11477

Read Online

ACCESS | Metrics & More | Article Recommendations | Supporting Information

ABSTRACT: Density functional theory (DFT) calculations are performed on the newly developed and designed photosensitizers having [D-D-triad-A]- and [D−π−π−A]-type structural models for near-infrared absorption dye-sensitized solar cells (DSSCs). For this purpose, three novel molecules are designed, which are named as follows: [naphthalene-anthracene-thiophene-furan-benzonitrile] as dye S1, [coronene-anthracene-thiophene-furan-benzonitrile] as dye S2, and [fluorene-thiophene-furan-benzonitrile] as dye S3. In all three systems, benzonitrile is the acceptor moiety, while thiophene and furan are bridging moieties. Naphthalene and anthracene are donor moieties in S1, whereas coronene and anthracene are donor moieties in S2, and fluorene is the only single donor moiety used for designing the dye complex S3. All three dye complexes are optimized under the DFT framework by using the B3LYP hybrid functional with 6-31G(d,p) basis set on Gaussian 16W software. The absorption spectra are calculated utilizing time-dependent density functional theory (TD-DFT) with the CAM-B3LYP/6-31G(d,p) basis set. The calculated absorption maxima of S1 and S2 are 749.45 and 750.04 nm, respectively, while for S3, it is reported to be at 337.35 nm, which suggests that the designed molecular structure having a double-donor moiety is suitable for high absorption wavelength. Further, the analysis of frontier molecular orbital energy gap suggests that the molecular systems S1, S2, and S3 have values 2.17, 2.13, and 3.618 eV, respectively, which lie in the semiconducting region. The other parameters calculated for the photovoltaic performance are exciton binding energy, change in free energy of charge regeneration, change in free energy of charge injection, oscillator strength, light harvesting efficiency, and open-circuit voltage.

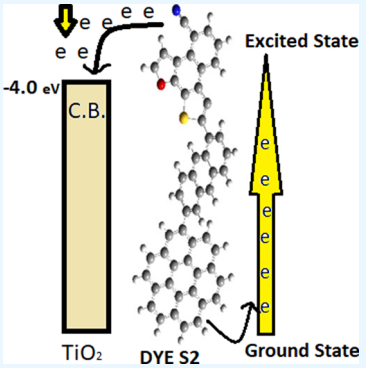

1. INTRODUCTION

The dye-sensitized solar cells can be fabricated on a flexible substrate and have a low production cost, which makes them environmentally friendly than inorganic material-based solar cells. Grätzel et al. made the first DSSC based on a ruthenium metal complex dye, which showed efficiency around 10%.[1] Since then, metal-free organic dyes are extensively explored in recent years.[2,3] The structures for designing the organic sensitizers for DSSC include donor, spacer, and acceptor units, all of which are connected together to form a dye molecule.[4,5] However, the other structures based on one donor and two acceptors [D−π−A−A], two donors and one acceptor [D−D−π−A], and two bridging units and one acceptor [D−π−π−A] are also utilized for making efficient sensitizers, which could show a wide absorption region.[6−8] Also, the molecular structures based on the [D−A−π−A] model are investigated by Liu et al.,[9] which showed efficiency in the range of 5−7%; similarly, Sharmoukh et al. investigated dye molecules showing efficiency around 5.5%.[10] In designing the dye molecule, the tunability of the absorption region of the sensitizer is the key factor, which can be achieved either by increasing the electron-donating strength or by increasing the effective bridging length or by increasing the electron acceptor strength.[11−14] The widely utilized donor compounds are based on carbazole, coronene, naphthalene, anthracene, phenothiazine, diphenylamine, coumarin, and so forth; the spacer or bridging compounds commonly utilized are thiophene, thiazole, pyrrole, furan, and so forth; and the acceptor molecules which are commonly utilized are fullerene derivatives like $PC_{61}BM$, $PC_{71}BM$, cyanoacetic acid, rhodamine N-acetic acid, naphthalimide, benzothiadiazole, benzonitrile, and so forth.[15−17] Recent progress in the field of organic solar cells with new π-conjugated polymers, small molecules (SMs), fullerene-free acceptors (FFAs),[18−20] together with the better device configurations, has shown significant improvement in power conversion efficiencies of dye-based solar cells in the range of 10 to 16%.[6,21] To design an efficient photovoltaic device, both the donor and acceptor materials play a crucial role. Hence, in this paper, we have focused on designing the near-infrared-

Received: October 17, 2023
Revised: February 7, 2024
Accepted: February 14, 2024
Published: February 28, 2024

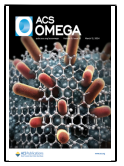

absorbing dyes which could show better device efficiency if synthesized. The designed two novel dyes S1 and S2 are based on (double-donor molecular units and double-bridging molecular units connected with one acceptor molecular unit), while the third novel dye S3 is based on only a single-donor molecular unit for understanding the effect of double-donor moieties on the absorption wavelength and then various electronic, chemical, and optical parameters along with the photovoltaic performance are analyzed. The various electronic and chemical parameters which are discussed in the paper are frontier molecular energy orbitals like HOMO and LUMO energy levels, HLG gap energy, ionization potential, electron affinity, and further the optical and photovoltaic parameters like excitation energy, exciton binding energy, maximum absorption wavelength, dye regeneration driving force or change in free energy of dye regeneration, change in free energy of charge injection, oscillator strength, and open-circuit voltage for the designed dyes.

We have utilized a [D-D-triad-A] molecular structure approach to design near-infrared-absorbing dyes and one dye complex with just one single-donor moiety [D−π−π−A] structure for understanding the effect of double donor moiety in comparison to the single donor moiety on the photosensitizer efficiency. The donor moieties for system S1 are naphthalene and anthracene, which are chosen because of the coplanarity of acene molecules, which results in efficient charge transfer in the molecule. Similarly, system S2 has coronene and anthracene as donor units, which are coplanar in the geometrical arrangement. Further, the chosen bridging units are based on thiophene and furan units which are heteroaromatic molecules that could help in charge transfer from one end of the molecule to another end. One of the important aspects of designing an efficient photosensitizer is to choose a high electron affinity molecule as the electron acceptor unit. Therefore, we have used benzonitrile as the electron acceptor unit in all the designed systems due to its high electron affinity which will act as an electron puller from the donor site of the dye molecule and which is also expected to reduce the recombination process of the generated exciton pair at the donor-bridging interface.[22,23] The first system is named as S1 [naphthalene-anthracene-thiophene-furan-benzonitrile] and the second system is named as S2 [coronene-anthracene-thiophene-furan-benzonitrile], while the third system is named as S3 [fluorene-thiophene-furan-benzonitrile]. All the chemical compounds are expected to be prepared using the chemical solution method, and further the DSSC fabrication can be done using the doctor blade method.[24] All of the optimized dyes S1, S2, and S3 are shown in Figure 1. The designed molecules were targeted to show a high absorption wavelength for S1 and S2 dyes.

The charge-transfer mechanism in the dye-sensitized solar cells is divided into four steps: the first step is to absorb the light photons by the dye molecule; the second step is to separate the charge carriers generated due to the absorption of photonic energy; the third step is to transport this separated electron−hole toward the counter electrode; and the fourth step is to regenerate the dye molecule. In other words, the excited electron would be injected into the conduction band of the semiconducting material (e.g., TiO_2, SnO_2, ZnO, CuO, etc.), and then it is transferred to the external circuit. Further, the oxidized dye gets regenerated through the electrolyte solution (e.g., iodide solution), which is used as a filler in the dye-based solar cells. For an efficient charge transfer from the sensitizer, the LUMO levels of the dye must be at a higher position than the conduction band of the semiconducting material, and the HOMO levels of the dye must be at a lower level of the electrolyte's redox potential.[25,26]

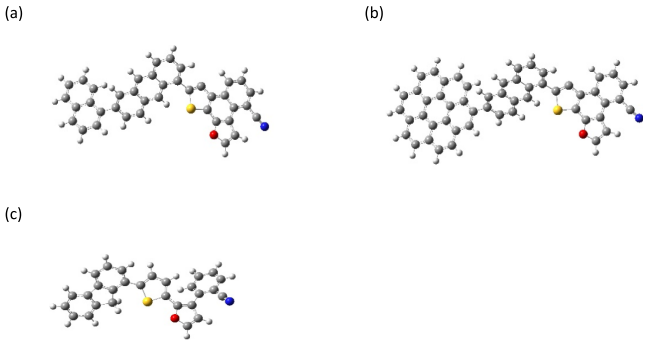

Figure 1. (a) Optimized geometry of S1 [naphthalene-anthracene-thiophene-furan-benzonitrile] at the B3LYP/6-31G(d,p) level. (b) Optimized geometry of S2 [coronene-anthracene-thiophene-furan-benzonitrile] at the B3LYP/6-31G(d,p) level. (c) Optimized geometry of S3 [fluorene-thiophene-furan-benzonitrile] at the B3LYP/6-31G(d,p) level.

2. COMPUTATIONAL DETAILS

All the three dye molecules were modeled on the Gauss View interface,[27] and then these are optimized using the density functional theory[28] at the B3LYP and 6-31G(d,p) level[29] on the Gaussian 16W package.[30] The density functional theory method has been extensively used in the theoretical studies of organic molecules with the B3LYP hybrid functional. The B3LYP hybrid functional has been chosen because of its most approximate optimization results when matched with the experimental values for organic molecules.[31−34] All of the calculations reported here are performed in the gas-phase environment. Further, the experimental verification of DFT calculation is discussed in the literature very well, which is reported by various authors.[35,36] Further, the molecules are also checked by frequency calculations to confirm the true global minima of the optimized systems. The vertical transition energy or absorption maxima is calculated using the TD-DFT method along with the long-range-corrected functional CAM-B3LYP/6-31G(d,p) level.[37] The other functional like LC-BLYP[38−40] for calculating excitation energies is also useful.

3. RESULTS AND DISCUSSION

To look for the effect of double-donor and double-bridging structures on the photovoltaic performance of the designed dyes, a proper selection of the donor and acceptor units is necessary for designing the photosensitizers. Apart from the simple D−π−A model, the introduction of additional donors and extension of π-conjugation length through the double-bridging molecule results in the reduction of the HOMO−LUMO energy gap and shows the high absorption maximum in the visible spectrum.

The frontier molecular orbital analysis for all the systems suggests that in the first dye (S1) structure, the HOMO is mostly spread over the donor and π-bridge molecular unit, i.e., the charge is spread over the naphthalene and anthracene units along with the thiophene and furan units, while the LUMO is found over the bridging molecular units, i.e., thiophene and furan molecules majorly. This suggests the electron-rich nature of the naphthalene and anthracene units as compared to the

https://doi.org/10.1021/acsomega.3c08165
ACS Omega 2024, 9, 11471−11477

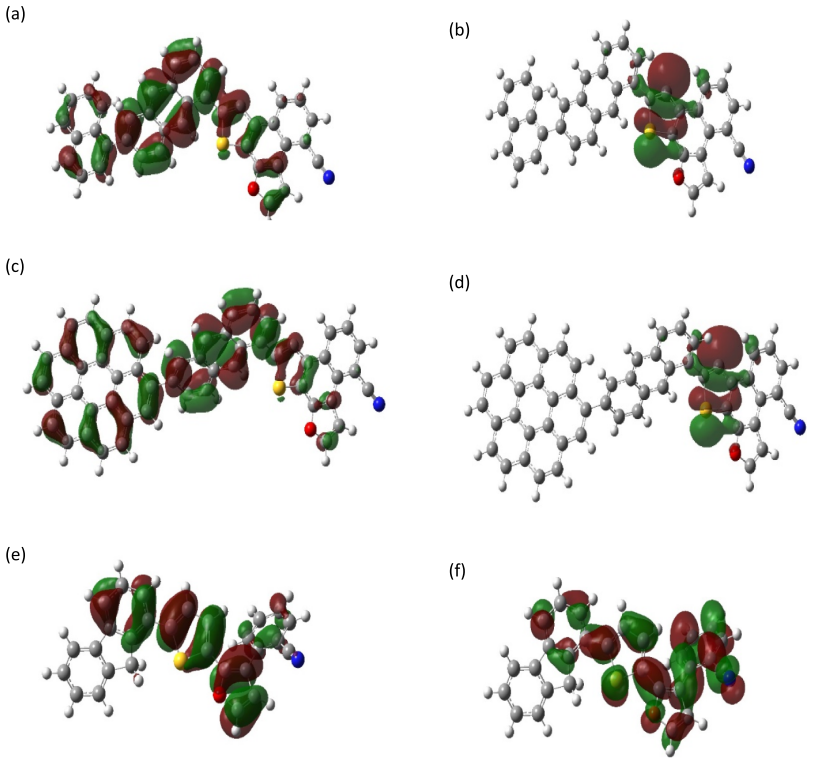

Figure 2. (a) HOMO charge distribution of S1 [naphthalene-anthracene-thiophene-furan-benzonitrile]; (b) LUMO charge distribution of S1 [naphthalene-anthracene-thiophene-furan-benzonitrile]; (c) HOMO charge distribution of S2 [coronene-anthracene-thiophene-furan-benzonitrile]; (d) LUMO charge distribution of S2 [coronene-anthracene-thiophene-furan-benzonitrile]; (e) HOMO charge distribution of S3 [fluorene-thiophene-furan-benzonitrile]; and (f) LUMO charge distribution of S3 [fluorene-thiophene-furan-benzonitrile] for the designed dyes in the ground state.

benzonitrile unit. Similarly, for the second molecular structure system (S2), the HOMO lies over the donor and bridging molecule, i.e., the coronene and anthracene units as donor site while thiophene and furan units as bridging sites, while LUMO lies majorly over the bridging unit, i.e., thiophene and furan units. For system (S3), the HOMO lies over the donor and bridging units and LUMO lies over the bridging and acceptor units. A small part of the LUMO also spreads over the benzonitrile unit in all the three molecular systems, which suggests that the charge separation is quite high in the ground state, which also confirms the asymmetric distribution of the charges in the ground state. The charge distribution of the HOMO and LUMO orbitals for all three molecules is shown in Figure 2.

The HLG energies for systems S1 and S2 calculated in the ground state are 2.173 and 2.139 eV, which suggest that both the molecules have low HLG energy. However, system S3 has a HLG energy at 3.618 eV. To have a high absorption maxima or wide absorption wavelength, it is a must that the HOMO−LUMO gap energy be very low, which can be achieved through the addition of donor units and bridging molecule units in the full dye structure. Herein, we have double-donor and double-bridging units in the dye structure for S1 and S2, which resulted in the lower HLG energy for both the systems.

Further, for the efficient charge transfer in the dye molecule, the HOMO of the dye molecule should be at a lower value than the redox potential of the electrolyte solution, while the LUMO level of the dye molecule must be at higher level than the conduction band edge of the semiconducting metal oxide, i.e., TiO_2 here. For the molecular system S1, the HOMO level of the dye molecule lies at −5.313 eV, and for system S2, the HOMO level lies at −5.289 eV. Similarly, for molecular system S3, the HOMO level lies at −5.374 eV. This confirms that the HOMO level of the designed dyes are at lower level than the redox potential of the electrolyte (iodide solution chosen here) which lies at −4.8 eV. Therefore, all the designed dyes are suitable for charge regeneration. The LUMO level for systems S1, S2, and S3 lies at −3.140 eV, −3.150 eV, and −1.756 eV, respectively. This confirms that the LUMO level lies at an upper level than the conduction band edge of TiO_2 at −4.0 eV. This is good enough for the charge transfer from the LUMO level of the dye to the TiO_2 conduction band. Also, the values of ionization potential and electron affinity are analyzed by using Koopman's approximation where the -HOMO energy represents the ionization potential, while the -LUMO energy represents the electron affinity. We have found electron affinity for both molecules S1 and S2 higher than 3 eV, which is good enough to extract the electron from the donor site. Therefore, the molecular structure having benzonitrile as the electron acceptor proves to be a good strategy to form a photosensitizer. The values are reported in Table 1.

The close alignment of the energy levels of the designed dyes with the photoanode is the result of an extra donor moiety available in the form of naphthalene in system S1 and as coronene in system S2 in comparison to the single-donor moiety used in the S3 system. The double-bridging unit has also played a key role in aligning the energy levels with the photoanode TiO_2. The extra donor unit helps in the increase of the conjugation length, which also improves the charge-transfer probability in the system. System S1 has naphthalene and anthracene as the donor units which are connected in a coplanar manner with each other that improves the energy

https://doi.org/10.1021/acsomega.3c08165
ACS Omega 2024, 9, 11471−11477

Table 1. HOMO, LUMO, HOMO−LUMO Energy Gap, Ionization Potential, Electron Affinity, and Exciton Binding Energy Values in eV

dyes	HOMO energy (eV)	LUMO energy (eV)	HLG energy (eV)	ionization potential (eV)	electron affinity (eV)	exciton binding energy (eV)
dye (S1)	−5.313	−3.140	2.173	5.313	3.140	0.519
dye (S2)	−5.289	−3.150	2.139	5.289	3.150	0.486
dye (S3)	−5.374	−1.756	3.618	5.374	1.756	−0.057

alignment with the photoanode material. The charge donating nature of the dye molecule is basically represented by the HOMO orbital while LUMO orbital of the dye molecule represents the charge accepting nature of the dye molecule, as reported in earlier studies by other authors.[31,41] The acceptor unit of benzonitrile when irradiated with sunlight, as reported in the literature, follows the breakage of the carbon−carbon bond between the aromatic ring and the CN group. This produces some intermediates that are strongly adsorbed over the TiO_2 surface. Therefore, the chosen acceptor moiety may be successful in transferring the charge to this semiconducting photoanode.[42]

3.1. Absorption Spectra. The calculated absorption spectra along with the oscillator strength, light-harvesting efficiency (LHE), and intramolecular charge-transfer excitation energy are obtained using the TD-DFT method at the CAM-B3LYP/6-31G(d, p) level of theory, whose values are reported in Table 2. We have chosen the CAM-B3LYP functional for calculating the absorption spectra due to its long-range correction available for the organic molecules. In designing a DSSC, the role of absorption spectra is very critical. For efficient light harvesting, the absorption maxima should be in the visible spectrum, and for the optimum utilization of visible spectrum, the dyes should be able to absorb mostly in the wavelength nearest to that of the red color. Therefore, the selection of donor and bridging units has become very important in designing an efficient photosensitizer. In the designed novel dyes, the first system S1 shows the absorption maxima at 749.45 nm, and the second system S2 shows the absorption maxima at 750.04 nm, which are reported in Table 2. Both the dyes show very high absorption maxima in the near-infrared region. The reason for this high absorption wavelength in both systems is attributed to their strong extended conjugation length which is due to the presence of double-donor units, while system S3 has absorption maxima at 337.35 nm which lies in the UV region because it has only one single unit of donor moiety in the form of fluorene. Therefore, it is suggested from the absorption wavelength results that a double-donor moiety is suitable for designing high absorption wavelength dyes. Further, the other parameters like LHE, oscillator strength, and intramolecular charge-transfer excitation energy are also reported in Table 2, which suggest that both systems S1 and S2 are closely related in terms of their values which is attributed to their molecular architecture. From this analysis of the absorption spectra, we can expect to utilize the [D-D-triad-A] molecular model to design a photosensitizer which may have a high absorption wavelength.

Table 2. Computed Maximum Absorption Wavelengths (λ_{max}) in nm, Oscillator Strengths (f), Light-Harvesting Efficiency (LHE), and λ_{max}^{ICT} in eV Reported for Modeled Dye Sensitizers

dyes	absorption wavelengths (λ_{max}) (nm)	oscillator strengths (f)	LHE (eV)	λ_{max}^{ICT} in (eV)
dye (S1)	Exc.State first = 834.30	0.0000	0.0000	1.486
	Exc.State second = 749.45	0.0019	0.0044	1.654
	Exc.State third = 539.66	0.0001	0.0030	2.297
dye (S2)	Exc.State first = 835.43	0.0000	0.0000	1.484
	Exc.State second = 750.04	0.0021	0.0049	1.653
	Exc.State third = 622.58	0.0000	0.0000	1.991
dye (S3)	Exc.State first = 337.35	0.821	0.8489	3.675
	Exc.State second = 279.67	0.056	0.1209	4.433
	Exc.State third = 271.40	0.054	0.1169	4.568

3.2. Photovoltaic Properties. The photovoltaic parameters calculated for the designed dyes are light-harvesting efficiency, change in free energy of the charge injection, open-circuit voltage, change in free energy of charge regeneration, absorption maxima, excitation energy, and binding energy of the exciton pair.

The ground-state oxidation potential (E_{ox}^{dye}) of a dye can be approximated as the negative of the dye's HOMO energy ($-E_H$). Further, the excited-state dye regeneration driving force (ΔG_{reg}) can be approximated as ($-(E_H) - 4.8$) eV, where −4.8 eV stands for the redox potential of the I^-/I^{3-} electrolyte couple.[31,43]

The change in free energy of electron injection (ΔG_{inject}) from the excited state of the dye to the semiconductor TiO_2 is calculated as below[43]:

$$\Delta G_{(inject)} = E_{ox}^{dye*} - E_{CB}^{TiO_2}$$

where, E_{CB}^{TiO2} represents the conduction band energy of the TiO_2 material which has value = -4.0 eV. Here, we have taken the mod value of E_{CB}^{TiO2} , or more simplified formula of change in free energy of electron injection can be written as $\Delta G_{(inject)} = E_{ox}^{dye*} - 4.0$

E_{dye}^{*ox} is approximated as the difference between the ground-state oxidation potential of the dye and the absorption maxima energy,

$$E_{dye}^{*ox} = (-E_H) - \lambda_{max}$$

Further, the difference between the energy of the LUMO (E_L) of the dye and the energy of the conduction band edge of TiO_2 is regarded as the open-circuit voltage, $eV_{OC} = E_L - (-4.0)$. It is calculated as below:

$$V_{oc} = E_{LUMO}^{dye} - \text{C. B.}\ (E_{TiO_2})$$

The light-harvesting efficiency is calculated by using the following formula[44]:

$$LHE = 1 - 10^{-f}$$

Here, f represents the oscillator strength.

The exciton binding energy is one of the important aspects in designing photosensitizers. The effective charge separationis only possible when we have an exciton binding energy very small. It is defined as the difference between the neutral exciton pair energy and two free charge carriers, which is approximated by taking the difference between the electronic

https://doi.org/10.1021/acsomega.3c08165
ACS Omega 2024, 9, 11471−11477

and optical band gap energies of the photosensitizer. The electronic band gap is approximated as the difference between the HOMO and LUMO energy gaps, whereas the optical band gap is approximated as equal to the energy of the first singlet excitation state energy.[45] The values are collected in Table 1.

$$E_{(\text{binding energy of exciton pair})} = E_{(\text{HLG})} - E_{(\text{first singlet excitation energy})}$$

From Table 1, it is clearly visible that all the designed dyes have lower HOMO energy levels (i.e., for the first system, it is at −5.313 eV; for the second system, it is −5.289 eV; and for the third system, it lies at −5.374 eV) than the redox couple of the iodide solution (−4.8 eV), which confirms that the designed dyes will have fast regeneration.

The binding energies of the exciton pair for systems S1 and S2 are found to be very low, whose values are 0.519 and 0.486 eV, respectively, as compared to the widely utilized donor material, i.e., spiro-OMeTAD whose exciton binding energy is 0.87 eV. This suggests that the electron hole pairs generated in the newly designed photosensitizers can easily dissociate into free charge carriers which will further improve the electron charge transport toward the photoanode. However, the exciton binding energy for system S3 is reported to be −0.057 eV, which shows the unstable nature of the generated exciton pair.

Table 2 shows the photovoltaic properties calculated in terms of absorption wavelength for the two photosensitizers S1 and S2 which are from the second excited state whose values are at 749.45 and 750.04 nm, respectively; the oscillator strength of S1 and S2 are 0.0019 and 0.0021, respectively; the LHE values for the designed dyes are reported as 0.0044 and 0.0049 eV for the first system S1 and second system S2, respectively. We have neglected the other excited-state values due to their zero-oscillator strength or because they represent a lower oscillator strength than the second excited state. Further, the intramolecular charge-transfer energies for S1 and S2 are reported to be 1.654 and 1.653 eV, respectively. This suggests that the photovoltaic parameters calculated for both systems are quite similar to each other, which is due to their molecular architecture which is based on heavy donor units [D−D−π−π−A]. While the photosensitizer S3 has a low absorption wavelength at 337.35 nm, the first excited state has good oscillator strength at 0.821, which is why the LHE value for this dye molecule is higher as compared to that of the dyes S1 and S2.

In Table 3, the ΔG_{inject} (change in free energy of the charge injection) values calculated for systems S1, S2, and S3 are

Table 3. Computed $\Delta G_{(\text{inject})}$, $E_{\text{OX}}^{\text{dye}*}$, and $E_{\text{OX}}^{\text{dye}}$ of Dye (S1), Dye (S2), and Dye (S3) Sensitizers Calculated in Units of eV

dyes	$\Delta G_{(\text{inject})}$ energy (eV)	$E_{\text{OX}}^{\text{dye}*}$ energy (eV)	$E_{\text{OX}}^{\text{dye}}$ energy (eV)
dye (S1)	−0.341	3.659	5.313
dye (S2)	−0.364	3.636	5.289
dye (S3)	−2.301	1.699	5.374

shown to be −0.341, −0.364, and −2.301 eV, respectively, where all the three systems show negative values, which confirms that charge injection into the conduction level of the semiconducting material would be favorable. It is also desired to have rapid electron injection from the dye molecule to the photoanode material, which is TiO_2 here. More the value becomes negative for ΔG_{inject}, the better will be the charge injection efficiency. In our system, for both molecules S1 and S2, the ΔG_{inject} values are very close in magnitude to each other, while the S3 dye complex has a higher charge injection value. This suggests that all the designed dye complexes will have an efficient charge injection rate. Here, the other parameters calculated are the oxidized energy of the dye in the excited state and in the ground state denoted by $E_{\text{OX}}^{\text{dye}*}$ and $E_{\text{OX}}^{\text{dye}}$, respectively.

From Table 4, the dye regeneration energy ΔG_{reg} calculated for the first system (S1) is found to be 0.51 eV; for the second

Table 4. Computed Dye Regeneration Energy $\Delta G_{(\text{reg})}$ and Open-Circuit Voltage V_{oc} (in eV) for All Dyes

dyes	regeneration energy $\Delta G_{(\text{reg})}$ (eV)	open-circuit voltage V_{oc} in (eV)
dye (S1)	0.51	0.86
dye (S2)	0.48	0.85
dye (S3)	0.57	2.25

system (S2), it is 0.48 eV, while for the third system (S3), it is 0.57 eV. All the dyes will be regenerated sharply due to their lower regeneration energy. We can also confirm that the second dye will regenerate faster due to its lower regeneration energy as compared to the first and third dyes. While dyes S1 and S2 show very similar results which may be attributed to their resembling molecular structures, second molecule of the dye S2 has coronene as one of the donor units, while dye S1 has naphthalene as the donor unit, whereas anthracene is common in both the molecular systems.

Further, the open-circuit voltage for system S1 is 0.86 eV, and for system S2, it is 0.85 eV, while for S3, the open-circuit voltage value is reported to be 2.25 eV, which shows that dyes S1 and S2 have similar open-circuit voltage values. Therefore, in conclusion, it can be inferred that the designed dyes S1 and S2 show similar photovoltaic properties and could be useful in designing near-infrared or high absorption wavelength photosensitizers for the dye-sensitized solar cells.

4. CONCLUSIONS

In this study of novel dyes based on double-donor and double-bridging molecular units along with one acceptor molecular unit named as [D-D-triad-A] to form an efficient photosensitizer for DSSC, it is found that both the designed dyes S1 [naphthalene-anthracene-thiophene-furan-benzonitrile] and S2 [coronene-anthracene-thiophene-furan-benzonitrile] have shown low HLG energy at 2.173 and 2.139 eV, respectively, which resulted in a high absorption wavelength as compared to the dye S3 which is based on a single-donor unit [D−π−π−A]. All of the dyes S1, S2, and S3 have shown efficient photovoltaic performance. Also, we have found the exciton binding energies for both systems S1 and S2 which are reported to be 0.519 and 0.486 eV, respectively, which are lower than that of the well-known donor material spiro-OMeTAD whose exciton binding energy lies at 0.86 eV. This shows that our designed molecules will be far superior in dissociating the charge carriers. Further, the absorption wavelengths for S1 and S2 are calculated to be 749.45 and 750.04 nm, respectively, which lie in the near-infrared region of the visible spectrum. This high absorption may be the result of extended conjugation length which is present in both dyes due to the presence of double-donor molecular units in the designed dyes. From the space charge

https://doi.org/10.1021/acsomega.3c08165
ACS Omega 2024, 9, 11471−11477

distribution plots of HOMO and LUMO, it was found that HOMOs representing the electron-rich nature were found over the donor and bridging sites, while LUMO which represents the unoccupied energy levels of electrons was found majorly over the thiophene and furan units in all the dyes, which showed that charge transfer is favorable from the donor to acceptor site through the bridging unit. Therefore, we expect that this study based on the [D-D-triad-A] molecular architecture would be helpful in designing efficient photosensitizers which could show absorption in the near-infrared region for DSSCs.

■ ASSOCIATED CONTENT

Data Availability Statement

All data included and analyzed in the manuscript.

Supporting Information

The Supporting Information is available free of charge at https://pubs.acs.org/doi/10.1021/acsomega.3c08165.

Natural transition orbitals for all three dye complexes and geometrically optimized coordinates for all three dyes (PDF).

■ AUTHOR INFORMATION

Corresponding Authors

Rudra Sankar Dhar − *Department of Electronics and Communication Engineering, NIT Mizoram, Aizawl 796012, India;* orcid.org/0000-0002-6571-3808; Email: rudra.ece@nitmz.ac.in

Na'il Saleh − *Department of Chemistry, College of Science, United Arab Emirates University, Al Ain 15551, United Arab Emirates;* orcid.org/0000-0003-3282-1156; Email: n.saleh@uaeu.ac.ae

Authors

Ankit Kargeti − *Department of Electronics and Communication Engineering, NIT Mizoram, Aizawl 796012, India; Department of Applied Sciences, School of Engineering and Technology, BML Munjal University, Gurugram, Haryana, NCR 122413, India;* orcid.org/0000-0002-7424-0651

Shamoon Ahmad Siddiqui − *Department of Physics, Integral University, Lucknow, Uttar Pradesh 226026, India*

Complete contact information is available at: https://pubs.acs.org/10.1021/acsomega.3c08165

Author Contributions

A.K., R.S.D., and S.A.S. did the conceptualization and conducted experiments, formal analytical investigations and modeling, validation and software, methodology, analyzed the data and wrote the main manuscript text, and prepared the figures. R.S.D. and S.A.S. supervised and initiated the research study and suggested improvements to the manuscript. R.S.D. and N.S. initiated the project administration and funding acquisition. A.K., R.SD., and S.A.S. discussed the results and contributed to the original draft preparation. All authors formulated the methods and design and reviewed the manuscript. All authors reviewed the manuscript and agreed to the final version. R.S.D. and N.S. are the corresponding authors.

Funding

This research received no external funding.

Notes

The authors declare no competing financial interest.

■ ACKNOWLEDGMENTS

The authors would like to thank UAE University for sponsoring the project (Grant # 12S106). All authors also thank the ECE Department, NIT Mizoram, India. S.A.S. is thankful to the Deanship of Research and Development, Integral University, Lucknow, Uttar Pradesh, India, for providing manuscript communication number (MCN): IU/R & D/2024-MCN0002327.

■ REFERENCES

(1) O'Regan, B.; Grätzel, M. A low-cost, high efficiency solar cell based on dye-sensitized colloidal TiO2 films. *Nature* **1991**, *354*, 56−58.

(2) Unny, D.; Sivanadanam, J.; Mandal, S.; Aidhen, I. S.; Ramanujam, K. Effect of Flexible, Rigid Planar and Non-Planar Donors on the Performance of Dye-Sensitized Solar Cells. *J. Electrochem Soc.* **2018**, *165*, H845−H860, DOI: 10.1149/2.0551813jes.

(3) Lai, F.; Yang, J.; Hsu, Y.; Lin, K.; Kuo, S. Enhancing DSSC Performance through Manipulation of the Size of ZnO Nanorods. *ACS Omega.* **2023**, *8* (43), 40206−20211.

(4) Mishra, A.; Fischer, M. K. R.; Büuerle, P. Metal-Free organic dyes for dye-Sensitized solar cells: From structure: Property relationships to design rules. *Angew. Chem., Int. Ed.* **2009**, *48* (14), 2474−2499.

(5) Liu, W.; Li, H.; Huo, Y.; Yao, Q.; Duan, W. Recent Progress in Research on [2.2]Paracyclophane-Based Dyes. *Molecules.* **2023**, *28* (7), 2891.

(6) Mathew, S.; Yella, A.; Gao, P.; et al. Dye-sensitized solar cells with 13% efficiency achieved through the molecular engineering of porphyrin sensitizers. *Nat. Chem.* **2014**, *6* (3), 242−247.

(7) Ricks, A. B.; Solomon, G. C.; Colvin, M. T.; et al. Controlling electron transfer in donor-bridge-acceptor molecules using cross-conjugated bridges. *J. Am. Chem. Soc.* **2010**, *132* (43), 15427−15434.

(8) Dessì, A.; Sinicropi, A.; Mohammadpourasl, S.; et al. New Blue Donor-Acceptor Pechmann Dyes: Synthesis, Spectroscopic, Electrochemical, and Computational Studies. *ACS Omega.* **2019**, *4* (4), 7614−7627.

(9) Liu, P.; Sharmoukh, W.; Xu, B.; et al. Novel and Stable D-A-φ-A Dyes for Efficient Solid-State Dye-Sensitized Solar Cells. *ACS Omega.* **2017**, *2* (5), 1812−1819.

(10) Sharmoukh, W.; Cong, J.; Ali, B. A.; Allam, N. K.; Kloo, L. Comparison between Benzothiadizole-Thiophene-and Benzothiadizole-Furan-Based D-A-Ï€-A Dyes Applied in Dye-Sensitized Solar Cells: Experimental and Theoretical Insights. *ACS Omega.* **2020**, *5* (27), 16856−16864.

(11) Koyyada, G.; Kumar Chitumalla, R.; Thogiti, S.; Kim, J. H.; Jang, J.; Chandrasekharam, M.; Jung, J. H.; et al. A new series of EDOT based co-sensitizers for enhanced efficiency of cocktail DSSC: A comparative study of two different anchoring groups. *Molecules* **2019**, *24*, 3554 DOI: 10.3390/molecules24193554.

(12) Li, G.; Jiang, K. J.; Li, Y. F.; Li, S. L.; Yang, L. M. Efficient structural modification of triphenylamine-based organic dyes for dye-sensitized solar cells. *J. Phys. Chem. C* **2008**, *112*, 11591.

(13) Manoharan, S.; Anandan, S. Cyanovinyl substituted benzimidazole based (D-π-A) organic dyes for fabrication of dye sensitized solar cells. *Dye Pigment. Published online* **2014**, *105*, 223.

(14) Sengul, O.; Boydas, E. B.; Pastore, M.; et al. Probing optical properties of thiophene derivatives for two-photon absorption. *Theor. Chem. Acc.* **2017**, *136* (6), 1−9.

(15) Namuangruk, S.; Jungsuttiwong, S.; Kungwan, N.; et al. Coumarin-based donor−π−acceptor organic dyes for a dye-sensitized solar cell: photophysical properties and electron injection mechanism. *Theor. Chem. Acc.* **2016**, *135* (1), 1−13.

(16) Chen, C. Y.; Wang, M.; Li, J. Y.; et al. Highly efficient light-harvesting ruthenium sensitizer for thin-film dye-sensitized solar cells. *ACS Nano* **2009**, *3* (10), 3103−3109.
(17) Fitri, A.; Benjelloun, A. T.; Benzakour, M.; McHarfi, M.; Hamidi, M.; Bouachrine, M. Theoretical investigation of new thiazolothiazole-based D-π-A organic dyes for efficient dye-sensitized solar cell. *Spectrochim. Acta - Part A Mol. Biomol. Spectrosc.* **2014**, *124*, 646−654.
(18) Ali, B.; Siddique, S. A.; Ahmed Siddique, M. B.; Ullah, S.; Ali, M. A.; Rauf, A.; Kamran, M. A.; Arshad, M. Insight on the structural, electronic and optical properties of Zn, Ga-doped/dual-doped graphitic carbon nitride for visible-light applications. *J. Mol. Graph Model.* **2023**, *125*, No. 108603.
(19) Facchetti, A. Polymer donor-polymer acceptor (all-polymer) solar cells. *Mater. Today.* **2013**, *16* (4), 123−132.
(20) Yan, C.; Barlow, S.; Wang, Z.; et al. Non-fullerene acceptors for organic solar cells. *Nat. Rev. Mater.* **2018**, *3*, 18003.
(21) Cui, Y.; Yao, H.; Zhang, J.; et al. Over 16% efficiency organic photovoltaic cells enabled by a chlorinated acceptor with increased open-circuit voltages. *Nat. Commun.* **2019**, *10* (1), 1−8.
(22) Selopal, G. S.; Wu, H. P.; Lu, J.; et al. Metal-free organic dyes for TiO2 and ZnO dye-sensitized solar cells. *Sci. Rep.* **2016**, *6*, 18756.
(23) Zhang, M.; Wang, Y.; Xu, M.; Ma, W.; Li, R.; Wang, P. Design of high-efficiency organic dyes for titania solar cells based on the chromophoric core of cyclopentadithiophene-benzothiadiazole. *Energy Environ. Sci.* **2013**, *6* (10), 2944−2949.
(24) Abrol, S. A.; Bhargava, C.; Sharma, P. K. Fabrication of DSSC using doctor blades method incorporating polymer electrolytes. *Mater. Res. Express.* **2021**, *8* (4), No. 045010.
(25) Gong, J.; Sumathy, K.; Qiao, Q.; Zhou, Z. Review on dye-sensitized solar cells (DSSCs): Advanced techniques and research trends. *Renew Sustain Energy Rev.* **2017**, *68*, 234−246.
(26) Fan, W.; Tan, D.; Deng, W. Q. Acene-modified triphenylamine dyes for dye-sensitized solar cells: A computational study. *ChemPhysChem* **2012**, *13*, 2051.
(27) Dennington, R.; Keith, T. A.; Millam, J. M. *GaussView, Version 6*; Semichem Inc.: Shawnee Mission, KS, 2016. GaussView 6. *Gaussian*. 2016.
(28) Kohn, W.; Sham, L. J. Self-consistent equations including exchange and correlation effects. *Phys. Rev.* **1965**, *140*, A1133 DOI: 10.1103/PhysRev.140.A1133.
(29) Becke, A. D. A new mixing of Hartree-Fock and local density-functional theories. *J. Chem. Phys.* **1993**, *98* (2), 1372−1377.
(30) Frisch, M. J., Trucks, G. W., Schlegel, H. E.et al.*Gaussian 16*; Gaussian, Inc: Wallingford CT, 2016.
(31) Divya, V. V.; Suresh, C. H. Density functional theory study on the donating strength of donor systems in dye-sensitized solar cells. *New J. Chem.* **2020**, *44* (17), 7200−7209.
(32) Siddiqui, S. A. Molecular modelling and simulation for the design of molecular diodes using density functional theory. *Mol. Simul.* **2020**, *46* (6), 460−467.
(33) Siddiqui, S. A.; Al-Hajry, A.; Al-Assiri, M. S. Ab initio investigation of 2,2′-bis(4-trifluoromethylphenyl)-5,5′-bithiazole for the design of efficient organic field-effect transistors. *Int. J. Quantum Chem.* **2016**, *116* (5), 339−345.
(34) Kargeti, A.; Rasheed, T.; Ahmad Siddiqui, S. Utilization of asymmetrical electron transport as strategy for modelling and design of efficient single molecule diodes: A DFT investigation. *Comput. Theor. Chem.* **2021**, *1205*, No. 113441.
(35) Paek, S.; Zimmermann, I.; Gao, P.; Gratia, P.; Rakstys, K.; Grancini, G. Chemical Science Donor − p − donor type hole transporting materials: marked p -bridge e ff ects on optoelectronic. *Chem. Sci.* **2016**, *7*, 6068−6075.
(36) Martín, N.; Segura, J. L.; Seoane, C. Design and synthesis of TCNQ and DCNQI type electron acceptor molecules as precursors for "organic metals. *J. Mater. Chem.* **1997**, *7* (9), 1661−1676.
(37) Jin, R.; Ahmad, I. Theoretical study on photophysical properties of multifunctional star - shaped molecules with 1, 8 - naphthalimide core for organic light - emitting diode and organic solar cell application. *Theor. Chem. Acc.* **2015**, *134*, 89 DOI: 10.1007/s00214-015-1693-8.
(38) Raeber, A. E.; Wong, B. M. The importance of short- and long-range exchange on various excited state properties of DNA monomers, stacked complexes, and Watson-Crick pairs. *J. Chem. Theory Comput.* **2015**, *11* (5), 2199−2209.
(39) Wong, B. M.; Hsieh, T. H. Optoelectronic and excitonic properties of oligoacenes: Substantial improvements from range-separated time-dependent density functional theory. *J. Chem. Theory Comput.* **2010**, *6* (12), 3704−3712.
(40) Ahn, D. H.; Song, J. W. Assessment of long-range corrected density functional theory on the absorption and vibrationally resolved fluorescence spectrum of carbon nanobelts. *J. Comput. Chem.* **2021**, *42* (7), 505−515.
(41) Jungsuttiwong, S.; Tarsang, R.; Sudyoadsuk, T.; Promarak, V.; Khongpracha, P.; Namuangruk, S. Theoretical study on novel double donor-based dyes used in high efficient dye-sensitized solar cells: The application of TDDFT study to the electron injection process. *Org. Electron.* **2013**, *14*, 711.
(42) Marcì, G.; Di Paola, A.; García-López, E.; Palmisano, L. Photocatalytic oxidation mechanism of benzonitrile in aqueous suspensions of titanium dioxide. *Catal. Today* **2007**, *129* (1−2), 16−21.
(43) Siddiqui, S. A. Molecular modeling and simulation for the design of dye sensitizers with mono- and di-substituted donor moieties. *J. Comput. Electron.* **2022**, *21* (1), 52−60.
(44) Rasheed, T.; Kargeti, A.; Siddiqui, S. A. Design of two novel dyes having maximum absorption in infrared region: A DFT investigation. *Mater. Today Proc.* **2022**, *68*, 2715−2719.
(45) Xu, Y. L.; Ding, W. L.; Sun, Z. Z. How to design more efficient hole-transporting materials for perovskite solar cells? Rational tailoring of the triphenylamine-based electron donor. *Nanoscale.* **2018**, *10* (43), 20329−20338.

https://doi.org/10.1021/acsomega.3c08165
ACS Omega 2024, 9, 11471−11477